Plane wave diffraction on a cylinder: WKB series combined with the asymptotic approximation near tangency points using the Pekeris caret function

Dmitry Ponomarev[1,2,3]

1 Introduction

In this note, we illustrate how two asymptotical methods can be combined to lay a foundation for an asymptotically convergent numerical scheme. We focus on a canonical case of scatterer with the circular cross-section, though the approach extends to other geometries of similar structure, i.e. convex bounded domains with 2 tangency points.

2 Formulation

We consider an exterior two-dimensional problem of plain wave scattering / diffraction by a smooth obstacle Ω in high-frequency regime ($k \gg 1$):

$$\Delta u + k^2 u = 0, \quad x \equiv (x_1, x_2) \in \mathbb{R}^2 \backslash \overline{\Omega}, \qquad u(x) = 0, \quad x \in \partial\Omega, \tag{1}$$

$$r^{1/2} \left| (\partial_r - ik) \left(u(x) - e^{ikx_1} \right) \right| \to 0 \quad \text{as} \quad r := |x| \to \infty. \tag{2}$$

Aiming at development of an efficient hybrid asymptotical-numerical method for high frequencies, we want to construct asymptotic representation of the solution which is uniformly accurate in the whole domain $\mathbb{R}^2 \backslash \overline{\Omega}$ as $k \to \infty$.

Denoting $u_i := e^{ikx_1}$, $u_s := u - u_i$, with help of the Green identities, one can derive an integral representation for the solution (i.e. total field) in terms of restriction of its normal derivative onto the obstacle boundary (see e.g. [3, 4])

$$u(x) = u_i(x) + \int_{\partial\Omega} G(x, y)\, \partial_n u(y)\, dy, \quad x \in \mathbb{R}^2 \backslash \overline{\Omega}, \tag{3}$$

[1]Institute of Analysis and Scientific Computing, Vienna University of Technology (TU Wien), Austria
[2]St. Petersburg Department of Steklov Mathematical Institute of Russian Academy of Sciences, Russia
[3]Contact: dmitry.ponomarev@asc.tuwien.ac.at

where $G(x,y) := -\frac{i}{4}H_0^1(k(|x-y|))$ is the scaled Hankel function of first kind, and $\partial_n u = n \cdot \nabla u$ with n being the unit normal vector on $\partial\Omega$ directed outwards with respect to Ω.

Representation (3) implies that it is enough to obtain sufficiently good approximation of the solution on the obstacle boundary $\partial\Omega$ in order to approximate the solution in the entire domain. Namely, in view of large-argument asymptotics of Hankel functions $H_0^{(1)}(z) = \sqrt{\frac{2}{\pi z}}e^{i(z-\pi/4)}$ for $|z| \gg 1$, application of the Cauchy-Schwarz inequality shows that the approximation error $\mathcal{E} := u - u_{\text{appr}}$ can be controlled as

$$\|\mathcal{E}\|_{L^\infty(\Omega)} \leq Ck^{-1/2}\|\partial_n \mathcal{E}\|_{L^2(\partial\Omega)} \tag{4}$$

with some $C > 0$ independent of k.

3 Exact solution

To understand the situation better, we take $\Omega = \mathbb{D}_{R_0} := \{(x,y) = (r\cos\theta, r\sin\theta) : r \in [0,R_0), \theta \in [0,2\pi)\}$, a disk of radius R_0 located at the origin.

In this case, on one hand, an explicit solution of (1)-(2) is readily available (though poorly converging for large kR_0, a fact that have prompted a lot of people to work on Watson transformation accelerating convergence) due to separation of variables and the cylindrical Jacobi-Anger expansion of the plane wave ($e^{ikr\cos\theta} = \sum_{n=-\infty}^{\infty} e^{in(\theta+\pi/2)}J_n(kr)$):

$$u(r,\theta) = e^{ikr\cos\theta} - \sum_{n=-\infty}^{\infty} \frac{J_n(kR_0)}{H_n^{(1)}(kR_0)} H_n^{(1)}(kr)\, e^{in(\theta+\pi/2)},$$

and, in particular, using $\left(H_n^{(1)}\right)'(z) = nH_n^{(1)}(z)/z - H_{n+1}^{(1)}(z)$, $z \in \mathbb{C}\backslash\{0\}$, $n \in \mathbb{N}_0$, we compute

$$\partial_n u(R_0,\theta) = -\frac{1}{R_0}\sum_{n=-\infty}^{\infty} J_n(kR_0)\left(n - \frac{H_{n+1}^{(1)}(kR_0)}{H_n^{(1)}(kR_0)}kR_0\right)e^{in(\theta+\pi/2)}. \tag{5}$$

4 Geometric optics solution

Following the geometric optics ansantz, we can write the scattered field $u_s = \mathcal{A}e^{ikS}$ and its 0th- and 1st-order approximations $u_0^s := \mathcal{A}_0 e^{ikS}$, $u_1^s := \left(\mathcal{A}_0 + \mathcal{A}_1\frac{1}{ik}\right)e^{ikS}$ with S, $\mathcal{A}_0$, $\mathcal{A}_1$ to be determined from (see e.g. [11])

$$|\nabla S| = 1, \quad x \in \mathbb{R}^2\backslash\overline{\Omega}, \qquad S(x) = x_1, \quad x \in \partial\Omega, \tag{6}$$

$$2\nabla S\cdot\nabla\mathcal{A}_0 + \mathcal{A}_0\Delta S = 0, \quad x \in \mathbb{R}^2\backslash\overline{\Omega}, \qquad \mathcal{A}_0(x) = -1, \quad x \in \partial\Omega, \tag{7}$$

$$2\nabla S\cdot\nabla\mathcal{A}_1+\mathcal{A}_1\Delta S=-\Delta\mathcal{A}_0,\quad x\in\mathbb{R}^2\backslash\overline{\Omega},\qquad \mathcal{A}_1(x)=0,\quad x\in\partial\Omega. \tag{8}$$

In case of our simple geometry, we have solutions to equations (6)-(8) which can be explicitly written in ray coordinates (σ,τ). Indeed, considering first the illuminated side, i.e. $\theta\in[\pi/2,3\pi/2]$, we introduce σ, τ so that

$$r=\sqrt{\sigma^2+R_0^2-2\sigma R_0\cos\tau},\quad \theta=\arctan\left(\frac{R_0\sin\tau-\sigma\sin 2\tau}{R_0\cos\tau-\sigma\cos 2\tau}\right)\quad \text{with } \theta=\tau \text{ for } \sigma=0.$$

Then, we have (see e.g. [11])

$$\mathcal{A}_0=-\sqrt{\frac{\cos\tau}{\cos\tau-2\sigma/R_0}},\quad S=\sigma+R_0\cos\tau,\quad \Delta S=\frac{2}{2\sigma-R_0\cos\tau}, \tag{9}$$

and, in particular, on the obstacle surface $\partial\Omega$:

$$\mathcal{A}_0|_{\sigma=0}=-1,\quad S|_{\sigma=0}=R_0\cos\theta,\quad \partial_n S=-\cos\theta,\quad \theta\in\left[\frac{\pi}{2},\frac{3\pi}{2}\right]. \tag{10}$$

Taking into account that

$$\nabla S\cdot\nabla\mathcal{A}_{0,1}=\frac{\partial\mathcal{A}_{0,1}}{\partial\sigma},\quad \partial_n\mathcal{A}_{0,1}|_{r=R_0}=\left.\frac{\partial\mathcal{A}_{0,1}}{\partial r}\right|_{r=R_0}=-\frac{1}{\cos\tau}\left.\frac{\partial\mathcal{A}_{0,1}}{\partial\sigma}\right|_{\sigma=0},$$

and computing $\Delta\mathcal{A}_0$ in ray coordinates, we obtain, from (7)-(8),

$$\partial_n\mathcal{A}_0|_{r=R_0}=\frac{1}{R_0\cos^2\theta},\quad \partial_n\mathcal{A}_1|_{r=R_0}=\frac{3\cos^2\theta-4}{R_0^2\cos^5\theta},\quad \theta\in\left[\frac{\pi}{2},\frac{3\pi}{2}\right]. \tag{11}$$

In the shadow region, $\theta\in[0,\pi/2)\cup(3\pi/2,2\pi)$, the ray coordinates (σ,τ) are such that

$$x_1=\sigma+R_0\cos\tau,\quad x_2=R_0\sin\tau,$$

and we have

$$S=\sigma+R_0\cos\tau=x_1,\quad \mathcal{A}_0\equiv-1,$$

which implies $\Delta S\equiv 0$ and $\mathcal{A}_1\equiv 0$ (and the same is true for all further order approximations, a fact that entails very good accuracy of the WKB series expansion in the shadow region making visible small effects of creeping waves which are not accounted here). Therefore, we finally conclude that, for $\theta\in(0,\pi/2)\cup(3\pi/2,2\pi]$,

$$S|_{r=R_0}=R_0\cos\theta,\quad \partial_n S|_{r=R_0}=\cos\theta,\quad \mathcal{A}_0|_{r=R_0}=-1,\quad \partial_n\mathcal{A}_0|_{r=R_0}=\partial_n\mathcal{A}_1|_{r=R_0}=0. \tag{12}$$

Employing (10), (11)-(12), let us now evaluate normal derivatives of approximations of the scattered field in the

illuminated and shadow regions.

$$\left.\frac{\partial u_1^s}{\partial r}\right|_{r=R_0} = \begin{cases} \left(ik\cos\theta + \dfrac{1}{R_0\cos^2\theta} + \dfrac{3\cos^2\theta - 4}{R_0^2\cos^5\theta}\dfrac{1}{ik}\right)e^{ikR_0\cos\theta}, & \theta \in \left[\dfrac{\pi}{2}, \dfrac{3\pi}{2}\right], \\ -ik\cos\theta e^{ikR_0\cos\theta}, & \theta \in [0, \pi/2) \cup (3\pi/2, 2\pi)\,, \end{cases} \tag{13}$$

and corresponding approximations to the total field derivatives

$$\partial_n u_1|_{r=R_0} = \begin{cases} \left(2ik\cos\theta + \dfrac{1}{R_0\cos^2\theta} + \dfrac{3\cos^2\theta - 4}{R_0^2\cos^5\theta}\dfrac{1}{ik}\right)e^{ikR_0\cos\theta}, & \theta \in \left[\dfrac{\pi}{2}, \dfrac{3\pi}{2}\right], \\ 0, & \theta \in [0, \pi/2) \cup (3\pi/2, 2\pi)\,. \end{cases} \tag{14}$$

Since the notion of order of approximation is different for the field and its normal derivative, we change terminology and, in further comparisons, we will call 0th-, 1st- and 2nd-order WKB approximation the expresions obtained by retaining one, two and, respectively, three first terms in (13)-(14).

5 Solution near the tangency points

We see that expressions (11) (and consequently (13)-(14)) blow up at $\theta = \pi/2,\ 3\pi/2$, this corresponds to inapplicability of the ray expansion. In fact, near the poles (which are intersections of the nonphysical caustic curve $\cos\tau = 2\sigma/R_0$, $\sigma < 0$ with the physical boundary $\sigma = 0$) the classical WKB expansion breaks down and another asymptotic approximation is needed. Such an approximation is furnished by Fock-Leontovich parabolic equation that can be first devised on physical grounds and then formalized by a modified WKB (Friedlander-Keller, see e.g. [1, 2, 6, 8, 9]) expansion. We give here a concise yet rather rigorous and essentially self-consistent derivation of the solution in the neighborhood of the tangency/diffraction points summarizing particular results and overall logic that can be found elsewhere [1, 2, 6, 7, 8, 9, 10].

Considering, for example, the north pole, i.e. the point $(x_1, x_2) = (0, R_0)$, let us search for the total field near $(r, \theta) = (R_0, \pi/2)$ in the form $u_{BL}(x_1, x_2) := e^{ikx_1}U(x_1, x_2)$ where

$$\partial_{x_1}^2 U + \partial_{x_2}^2 U + 2ik\partial_{x_1} U = 0. \tag{15}$$

The classical physical argument (see e.g. [1, 6]) goes that on the whole shadow boundary $x_2 = R_0$ the scattered field (after factoring out the incidence multiplier e^{ikx_1}) should undergo a drastical change in the vertical direction while being nearly constant in the horizontal one. This entails $\left|\partial_{x_1}^2 U\right| \ll \left|\partial_{x_2}^2 U\right|$ and hence results in what is known as parabolic wave-equation approximation:

$$\partial_{x_2}^2 U + 2ik\partial_{x_1} U = 0. \tag{16}$$

As a next step, we now approximate a part of the obstacle boundary $\partial\Omega$ near the north pole by a parabolic one (as the first-order expansion beyond the planar case): $x_2 = \sqrt{R_0^2 - x_1^2} \simeq R_0 - \dfrac{1}{2R_0}x_1^2$. Note that for a more general geometry, the first term here should be replaced with an ordinate of the tangency point and the local curvature should be used in place of $1/R_0$ in the second term).

Introducing new local coordinates $\tilde{\xi} := \alpha x_1$, $\tilde{\eta} := \beta\left(x_2 - R_0 + \dfrac{1}{2R_0}x_1^2\right)$, for some α, $\beta \in \mathbb{R}$, equation (16) becomes

$$\partial_{\tilde{\eta}}^2 U + \frac{2\alpha k}{\beta^2} i\left(\partial_{\tilde{\xi}} U + \frac{\beta}{\alpha^2 R_0}\tilde{\xi}\partial_{\tilde{\eta}} U\right) = 0$$

(note the abuse of notation $U \equiv U\left(\tilde{\xi},\tilde{\eta}\right) = U\left(x_1\left(\tilde{\xi},\tilde{\eta}\right), x_2\left(\tilde{\xi},\tilde{\eta}\right)\right)$).

In order to simplify coefficients, we choose the constants α, β such that $2\alpha k = \beta^2$, $\beta = \alpha^2 R_0$, and thus arrive at

$$\partial_{\tilde{\eta}}^2 U + i\left(\partial_{\tilde{\xi}} U + \tilde{\xi}\partial_{\tilde{\eta}} U\right) = 0 \tag{17}$$

with $\tilde{\xi} = (2kR_0)^{1/3} x_1/R_0$ and $\tilde{\eta} = (2kR_0)^{2/3}\left(x_2 - R_0 + \dfrac{1}{2R_0}x_1^2\right)/R_0$.

Note that after the performed change of variable, the parabolic boundary has become flat and is now described by an elementary equation $\tilde{\eta} = 0$.

Let us simplify equation (17) more by eliminating one of the derivatives. This can be done by transformation $U = e^{\psi} V$ with $\psi := \dfrac{i\tilde{\xi}}{2}\left(\dfrac{\tilde{\xi}^2}{6} - \tilde{\eta}\right) + \Theta\left(\tilde{\xi}\right)$ (a general form that eliminates first-order derivative in $\tilde{\eta}$) and V satisfying

$$\partial_{\tilde{\eta}}^2 V + i\partial_{\tilde{\xi}} V + \left(\frac{\tilde{\eta}}{2} + i\Theta'\left(\tilde{\xi}\right)\right) V = 0.$$

In particular, by taking $\Theta \equiv 0$, we have

$$\partial_{\tilde{\eta}}^2 V + i\partial_{\tilde{\xi}} V + \frac{1}{2}\tilde{\eta} V = 0,$$

and $U = \exp\left(\dfrac{i\tilde{\xi}}{2}\left(\dfrac{\tilde{\xi}^2}{6} - \tilde{\eta}\right)\right) V$, however, other choices of Θ will lead to different differential equations which might be also beneficial to consider.

Finally, we eliminate the factor $1/2$ by rescaling $\tilde{\xi} =: 2^{2/3}\xi$, $\tilde{\eta} =: 2^{1/3}\eta$, and thus arrive at

$$\partial_{\eta}^2 V + i\partial_{\xi} V + \eta V = 0 \tag{18}$$

and $U = \exp\left(i\left(\dfrac{\xi^3}{3} - \eta\xi\right)\right) V$ with $\xi = (k/2)^{1/3} x_1/R_0^{2/3}$, $\eta = (2/R_0)^{1/3} k^{2/3}\left(x_2 - R_0 + \dfrac{1}{2R_0}x_1^2\right)$.

Let us search solution to (18) in the Fourier form $V(\xi,\eta) = \int_{\mathbb{R}} e^{ip\xi}\hat{V}(p,\eta)\, dp$, we obtain

$$\partial_{\eta}^2 \hat{V} + (\eta - p)\hat{V} = 0. \tag{19}$$

Recall that the classical pairwise linear independent solutions to Airy equation

$$Y''(z) = zY(z)$$

are $\mathrm{Ai}(z)$, $\mathrm{Bi}(z)$, $\mathrm{Ai}\left(e^{\pm 2\pi i/3}z\right) = \frac{1}{2}e^{\pm \pi i/3}\left(\mathrm{Ai}(z) \mp i\mathrm{Bi}(z)\right)$, $z \in \mathbb{C}$. Note that each of these functions is entire.

Denoting $A_0(z) := \mathrm{Ai}(z)$, $A_1(z) := e^{2\pi i/3}\mathrm{Ai}\left(e^{2\pi i/3}z\right)$, we can thus write the general solution to (19) as

$$\hat{V}(p,\eta) = c_0(p)A_0(p-\eta) + c_1(p)A_1(p-\eta).$$

Boundary condition $u|_\Omega = 0$ implies $U|_{\eta=0} = V|_{\eta=0} = 0$, and therefore $c_1(p) = -c_0(p)A_0(p)/A_1(p)$ and

$$V(\xi,\eta) = \int_{\mathbb{R}} e^{ip\xi}c_0(p)\left(A_0(p-\eta) - \frac{A_0(p)}{A_1(p)}A_1(p-\eta)\right)dp. \tag{20}$$

It remains to determine the unknown function $c_0(p)$. A way to impose an appropriate "radiation condition" is to match at the leading order, for $\eta \to +\infty$, $\xi < 0$, the obtained boundary-layer solution

$$u_{BL} = e^{ikx_1}U(\xi,\eta), \quad \xi = \frac{k^{1/3}}{2^{1/3}R_0^{2/3}}x_1, \quad \eta = \frac{2^{1/3}k^{2/3}}{R_0^{1/3}}\left(x_2 - R_0 + \frac{1}{2R_0}x_1^2\right), \tag{21}$$

$$U(\xi,\eta) = e^{i\left(\frac{\xi^3}{3} - \eta\xi\right)}\int_{\mathbb{R}} e^{ip\xi}c_0(p)\left(A_0(p-\eta) - \frac{A_0(p)}{A_1(p)}A_1(p-\eta)\right)dp \tag{22}$$

to solution given by the classical (0th-order) WKB method which is valid in the illuminated region, i.e.

$$u_0 := u_i + u_0^s = e^{ikx_1} + \mathcal{A}_0 e^{ikS} \tag{23}$$

with $\mathcal{A}_0$, S as in (9).

To perform the matching, let us take $x_1 = -\delta_1 k^{-1/6}$, $x_2 = R_0 + \delta_2 k^{-1/3}$ for some arbitrary δ_1, $\delta_2 > 0$ independent of k. For values of x_1, x_2 of such an intermediate range we are, on the one hand, close to the tangency point so the boundary layer solution u_{BL} should be still valid, but, on the other hand, outside of the critical boundary layer so the classical WKB approximation furnishing geometric optics soltuion u_0 is expected to hold. All this is, of course, under the assumption that such a smooth transition is possible. This turns out to be the case here, and hence, by success of this matching procedure, we will be able to conclude that there are no intermediate boundary layers (which is, for example, not the case on the shadow side).

A complication that arises in this procedure is that the geometric optics solution (9) is given in terms of ray coordinates σ, τ which are not expressible in closed form in terms of the cartesian ones x_1, x_2 and hence neither in

terms of ξ, η. Instead, we only have

$$x_1 = R_0 \cos\tau - \sigma\cos 2\tau, \qquad x_2 = R_0 \sin\tau - \sigma \sin 2\tau, \qquad \sigma > 0, \quad \tau \in (\pi/2, 3\pi/2)\,. \tag{24}$$

However, since we need to perform matching only at the leading order of k, we can reduce complexity due to Taylor expansions. Note that the Jabobian of the transformation $(x_1, x_2) \mapsto (\sigma, \tau)$ degenerates at the point $(\sigma, \tau) = (0, \pi/2)$ making inverse function theorem not applicable, and hence we resort to a geometric argument (cf. [10]). As we know from solution procedure for eikonal equation, the rays are straight lines and hence for the point (x_1, x_2), there is a unique point (x_{01}, x_{02}) on the boundary (its parabolic approximation) upon which an incident ray reflects to approach (x_1, x_2), and the length of this segment is exactly a ray coordinate σ. It is geometrically clear that $(x_{01}, x_{02}) \to (0, R_0)$ as $(x_1, x_2) \to (0, R_0)$ for $k \to +\infty$. Because of Snell's law of reflection, the reflected ray has the direction

$$\tilde{d} = d - 2\,(n, d)\,n = \left(1 - 2\,(x_{01}/R_0)^2\,, -2x_{01}x_{02}/R_0^2\right)^T,$$

where $n = (x_{01}/R_0, x_{02}/R_0)^T$ is the unit normal vector at (x_{01}, x_{02}) and $d = (1, 0)^T$ is the incident direction. Taking into account $x_{02} \simeq R_0 - \frac{1}{2R_0}x_{01}^2$, the ray line equation $(x_1 - x_{01}, x_2 - x_{02})^T = \sigma\tilde{d}$ furnishes

$$\frac{x_2 - x_{02}}{x_1 - x_{01}} = \frac{-2x_{01}x_{02}/R_0^2}{1 - 2x_{01}^2/R^2} \simeq -\frac{2x_{01}/R}{1 - 2x_{01}^2/R_0^2}$$

$$\Rightarrow \quad x_{01} = \frac{1}{2}\left(x_1 - \sqrt{x_1^2 + 2R_0\,(x_2 - R_0)}\right) \simeq -\frac{1}{2}k^{-1/6}\left(\delta_1 + \sqrt{\delta_1^2 + 2R_0\delta_2}\right)$$

where the minus sign in front of the square root was chosen due to negativity of x_{01}.

The ray line equation and the last computation also imply

$$\sigma = \sqrt{(x_1 - x_{01})^2 + (x_2 - x_{02})^2} \simeq -\frac{(x_2 - R_0)\,R_0}{2x_{01}} = \frac{\delta_2 R_0}{\delta_1 + \sqrt{\delta_1^2 + 2R_0\delta_2}}k^{-1/6}. \tag{25}$$

From the first equation of (24)

$$2\sigma\cos^2\tau - R_0\cos\tau + x_1 - \sigma = 0$$

$$\Rightarrow \quad \cos\tau = \frac{1}{4\sigma}\left(R_0 - \sqrt{R_0^2 + 8\sigma\,(\sigma - x_1)}\right) \simeq (x_1 - \sigma)\,/R_0 \tag{26}$$

where the minus sign in front of the square root was due to the *a priori* known range $\tau \in (\pi/2, 3\pi/2)$.

Plugging (25)-(26) into (9) and further in (23), we arrive at

$$\mathcal{A}_0 = -\left(1 - 2\sigma/\left(R_0\cos\tau\right)\right)^{-1/2} = -\sqrt{\frac{x_1 - \sigma}{x_1 - 3\sigma}} = -\sqrt{\frac{\delta_1\left(\delta_1 + \sqrt{\delta_1^2 + 2R_0\delta_2}\right) + \delta_2 R_0}{\delta_1\left(\delta_1 + \sqrt{\delta_1^2 + 2R_0\delta_2}\right) + 3\delta_2 R_0}},$$

$$S = \sigma + R_0\cos\tau = x_1 = -\delta_1 k^{-1/6},$$

$$u_0 = e^{-ik\delta_1 k^{-1/6}} \left(1 - \sqrt{\frac{\delta_1 \left(\delta_1 + \sqrt{\delta_1^2 + 2R_0\delta_2} \right) + \delta_2 R_0}{\delta_1 \left(\delta_1 + \sqrt{\delta_1^2 + 2R_0\delta_2} \right) + 3\delta_2 R_0}} \right). \tag{27}$$

To compare this solution to the boundary-layer solution (21), we now turn to study the asymptotic behavior of the integral in (22) as $\eta \to +\infty$.

Let us make a mild *a priori* assumption on yet unknown function $c_0(p)$: suppose that it can be analytically continued from the negative axis into a (small) sector: $\{(r,\theta) : r \geq 0, \theta \in [\pi - \Delta]\}$ for some $0 < \Delta < \pi/3$, and its potential asymptotical growth there at infinity is $\mathcal{O}\left(\exp\left(\frac{2}{3}|p|^{2/3-q}\cos(\pi-\theta)\right)\right)$ for some $q > 0$.

Under such assumption, by Cauchy theorem, we can deform the contour from the negative real axis towards the halfline $\left\{re^{i(\pi-\Delta)}, r > 0\right\}$ and call the resulting contour Γ. The advantage of such contour deformation is that the integrand now decays exponentially at infinity along the both elements of the contour $\Gamma_1 := \left\{re^{i(\pi-\Delta)}, r > 0\right\}$, $\Gamma_2 := \left\{re^{i0}, r > 0\right\}$. Indeed, along Γ_2, we have exponential decay of $A_0(p-\eta)\left[1 - \frac{A_0(p)A_1(p-\eta)}{A_1(p)A_0(p-\eta)}\right]$ due to $A_0(p) = \mathcal{O}\left(p^{-1/4}\exp\left(-\frac{2}{3}p^{3/2}\right)\right)$, whereas, along Γ_1, the integrand $\frac{1}{A_1(p)}\left[A_1(p)A_0(p-\eta) - A_0(p)A_1(p-\eta)\right]$ decays due to the exponential growth of A_1: $A_1(p) = \mathcal{O}\left(|p|^{-1/4}\exp\left(-\frac{2}{3}|p|^{3/2}\cos\Delta\right)\right)$. Note that the actual decay rate is even better in view of the asymptotically vanishing factor in the square brackets. Due to the rapid decay of the integrand, we can truncate the integral contour Γ to finite limits commiting only an exponentially small error. We denote the resulting reduced contour as Γ^r and its parts in the left and right halfplane as Γ_1^r and Γ_2^r, respectively. We can now split the integral in (22) and study separately asymptotic behavior of the integrals, as $\eta \to +\infty$, $\xi < 0$,

$$I_1 := \int_{\Gamma^r} e^{ip\xi} c_0(p) A_0(p-\eta)\, dp, \qquad I_2 := \int_{\Gamma^r} e^{ip\xi} c_0(p) \frac{A_0(p)}{A_1(p)} A_1(p-\eta)\, dp.$$

Rigorous asymptotic estimates of both of these integrals can be efficiently obtained, at least in the region $\eta - \xi^2 = \mathcal{O}(1)$, $\xi < 0$, by the use of stationary phase method, but generally it is not a trivial matter and it will be skipped for the moment. The principal outcome of these computations, according to [7], is that $c_0(p) \equiv 1$.

Inserting it back into (22), we obtain consequently from (21)

$$u_{BL} = e^{i\left(\frac{\xi^3}{3} - \eta\xi + kx_1\right)} \int_{\mathbb{R}} e^{is\xi} \left(A_0(s-\eta) - \frac{A_0(s)}{A_1(s)} A_1(s-\eta) \right) ds. \tag{28}$$

This equation can be readily used for computation of the total field and, by substracting u_i, the scattered field as well. However, one can derive a direct integral form for it invoking the (distributional) Fourier transform of Airy function

$$\int_{\mathbb{R}} e^{-isz} \mathrm{Ai}(s)\, ds = e^{iz^3/3} \quad \Rightarrow \quad \int_{\mathbb{R}} e^{is\xi} A_0(s-\eta)\, ds = e^{i\eta\xi} \int_{\mathbb{R}} e^{is\xi} A_0(s)\, ds = e^{i\left(\eta\xi - \xi^3/3\right)}. \tag{29}$$

Therefore, the scattered field near the tangency point is furnished by

$$u_{BL}^{s} = -e^{i\left(\frac{\xi^3}{3}-\eta\xi+kx_1\right)} \int_{\mathbb{R}} e^{is\xi} \frac{A_0(s)}{A_1(s)} A_1(s-\eta)\, ds. \tag{30}$$

Since the computation (29) was only formal (the right-hand sides were not L^2 functions), it is not surprising that the integral in (30) is not properly defined. This can be remedied by splitting the integral into two parts and deforming integration contour in each of the term according to the asymptotical behavior of Airy functions. A handy way to rewrite this regularization result is to introduce an auxiliary function $\hat{p}(z)$ termed as Pekeris caret function [7]

$$\hat{p}(z) = \frac{1}{2\pi}\left(\frac{1}{it} + \int_{\Gamma_0} e^{izs}\frac{A_2(s)}{A_1(s)}ds - \int_0^{\infty} e^{izs}\frac{A_0(s)}{A_1(s)}ds\right), \quad z \in \mathbb{C},$$

where $\Gamma_0 := \left\{re^{2\pi i/3},\, r>0\right\}$, $A_2(s) := e^{-2\pi i/3}\mathrm{Ai}\left(e^{-2\pi i/3}s\right)$.

As can be seen, $\hat{p}$ is a meromorphic function whose only (single) pole is at the origin. It admits, besides other forms, the following useful integral representation [7]

$$\hat{p}(z) = -\frac{1}{4\pi z^2}\int_L \frac{\exp\left(e^{-i\pi/6}zs\right)}{\mathrm{Ai}^2(s)}ds, \quad z \in \mathbb{C}\backslash 0, \tag{31}$$

where L is any contour going from $\infty e^{-2\pi i/3}$ to $\infty e^{2\pi i/3}$ passing to the right of all zeros of Airy function $\mathrm{Ai}(s)$ situated on the negative real line (with the largest one at $s \simeq -2.3$).

Then, the scattered field (30) can be alternatively represented as

$$u_{BL}^{s} =: e^{ikx_1}U^s(\tilde{x}_1,\tilde{x}_2) = e^{ikx_1}\int_{\mathcal{L}} \hat{p}(s)\exp\left(i\left(s^3/3 - \tilde{x}_1 s^2/2 - \tilde{x}_2 s\right)\right)ds, \tag{32}$$

where $\mathcal{L}$ is a contour from $\infty e^{3\pi i/2}$ to $\infty e^{5\pi i/6}$ which neither touches nor encompasses the origin, and $\tilde{x}_1 := k^{1/3}(2/R_0)^{2/3}x_1$, $\tilde{x}_2 := k^{2/3}(2/R_0)^{1/3}(x_2 - R_0)$.

Let us now evaluate $\left.\dfrac{\partial u_{BL}^{s}}{\partial r}\right|_{r=R_0}$ near $\theta = \pi/2$

$$\begin{aligned}\left.\frac{\partial u_{BL}^{s}}{\partial r}\right|_{r=R_0} = \Bigg[&\frac{\partial U^s}{\partial \tilde{x}_1}\left(k^{1/3}\left(\frac{2}{R_0}\right)^{2/3}R_0\cos\theta,\; k^{2/3}\left(\frac{2}{R_0}\right)^{1/3}R_0(\sin\theta - 1)\right)k^{1/3}\left(\frac{2}{R_0}\right)^{2/3}\cos\theta \\ &+ \frac{\partial U^s}{\partial \tilde{x}_2}\left(k^{1/3}\left(\frac{2}{R_0}\right)^{2/3}R_0\cos\theta,\; k^{2/3}\left(\frac{2}{R_0}\right)^{1/3}R_0(\sin\theta - 1)\right)k^{2/3}\left(\frac{2}{R_0}\right)^{1/3}\sin\theta \\ &+ ik\cos\theta U^s\left(k^{1/3}\left(\frac{2}{R_0}\right)^{2/3}R_0\cos\theta,\; k^{2/3}\left(\frac{2}{R_0}\right)^{1/3}R_0(\sin\theta - 1)\right)\Bigg]e^{ikR_0\cos\theta},\end{aligned} \tag{33}$$

and, similarly, for the total field

$$\partial_n u_{BL}|_{r=R_0} = \left.\frac{\partial u_{BL}^{s}}{\partial r}\right|_{r=R_0} + ik\cos\theta e^{ikR_0\cos\theta}. \tag{34}$$

Finally, we note that for the other tangency point (i.e. the south pole: $(x_1, x_2) = (0, -R_0)$), the situation is absolutely analogous and can be obtained by symmetry replacing x_2 with $-x_2$, i.e. by working with the variables $\tilde{x}_2 = -k^{2/3}\left(2/R_0\right)^{1/3}(x_2 + R_0)$, $\tilde{\eta} = -\left(2kR_0\right)^{2/3}\left(x_2 + R_0 - \frac{1}{2R_0}x_1^2\right)/R_0$, $\eta = -\left(2/R_0\right)^{1/3}k^{2/3}\left(x_2 + R_0 - \frac{1}{2R_0}x_1^2\right)$ whereas $\tilde{x}_1$, $\tilde{\xi}$, ξ should be left unchanged.

6 Numerical implementation

As devised in the previous section (motivating the change of variables from (x_1, x_2) towards (ξ, η)), the size of the neighborhood, where the geometric optics theory breaks down, scales with wavenumber as $\mathcal{O}\left(\left(kR_0\right)^{-1/3}\right)$. On the other hand, it was noted that the boundary layer solution is valid in a slightly larger neighborhood (the fact that allowed to perform asymptotic matching). In a practical computation, we take $\delta := \left(kR_0\right)^{-1/3+1/9}$ as this "slightly larger neighborhood" (such choice of the size of the overlapping neighborhoods is also used in [5]) and use the derived boundary layer solution (33) for $\theta \in (\pi/2 - \delta, \pi/2 + \delta) \cup (3\pi/2 - \delta, 3\pi/2 + \delta)$ and geometrical optics solution (13)-(14) in the complementary region.

We have thus obtained an asymptotical solution that is globally valid on $\partial\Omega$ and, in view of (3)-(4), hopefully in the whole $\mathbb{R}^2\backslash\Omega$ as well. We will compare the this global asymptotical solution with the exact solution as given by (5).

Few remarks regarding numerical implementations should be made.

As it was already mentioned, the series for exact solution (5) converges badly for large values of k. To represent the field accurate enough, we increase, proportionally to k, the number of terms $M := 2kR_0$ in the series.

To compute Pekeris caret function, we use integral representation (31) with the contour $L = L_1 \cup L_2$ consisting of straight line segments. Namely, $L_1 := \left\{re^{-2\pi i/3},\, r > 0\right\}$, $L_2 := \left\{re^{2\pi i/3},\, r > 0\right\}$. For numerical computation, both rays L_1, L_2 were chopped at some $r_{m1} > 0$, and in the region $r > r_{a1}$ (for some $r_{a1} > 0$) the explicit large argument asymptotics of Airy function $\mathrm{Ai}(s) \simeq \frac{\exp\left(-3/2s^{3/2}\right)}{2\sqrt{\pi}s^{1/4}}$, $|s| \gg 1$ was used to facilitate numerical treatment of the exponentials.

In computing reflected field amplitude U^s entering the third term of (33), we choose the contour $\mathcal{L} = \mathcal{L}_1 \cup \mathcal{L}_2 \cup \mathcal{L}_3$ with $\mathcal{L}_1 := \left\{re^{3\pi i/2},\, r > r_0\right\}$, $\mathcal{L}_2 := \left\{r_0 e^{i\theta},\, \theta \in (5\pi/6, 3\pi/2)\right\}$, $\mathcal{L}_3 := \left\{re^{5\pi i/6},\, r > r_0\right\}$. As before, we truncate the rays $\mathcal{L}_1$, $\mathcal{L}_3$ at infinity at some $r_{m2} > 0$ and use analytical expression for Pekeris caret function $\hat{p}$ in the asymptotic regime $r > r_{a2}$ for some $r_{a2} > 0$, namely, $\hat{p}\,(s) \simeq \frac{\sqrt{-s}}{2\sqrt{\pi}} \exp\left[\frac{i}{4}\left(\pi - \frac{s^3}{3}\right)\right]$, $|s| \gg 1$. However, in the first two terms of (33), $\frac{\partial U^s}{\partial \tilde{x}_1}$, $\frac{\partial U^s}{\partial \tilde{x}_2}$ are computed using simple two-element contour consisting of only straight lines (again, numerically chopped at some r_{m2} and asymptotically approximated for $r > r_{a2}$) $\mathcal{L} = \tilde{\mathcal{L}}_1 \cup \tilde{\mathcal{L}}_3$, $\tilde{\mathcal{L}}_1 := \left\{re^{3\pi i/2},\, r > 0\right\}$, $\tilde{\mathcal{L}}_3 := \left\{re^{5\pi i/6},\, r > 0\right\}$. This simplification is possible due to the absense of the integrand singularity (the pole is cancelled by a derivative of the exponential, and such differentiation under the integral sign is justified by the absolute convergence of the integrals).

In the described contours L, $\mathcal{L}$, the mentioned parameters were chosen as $r_0 = 1$, $r_{m1} = 1000$, $r_{m2} = 100$, $r_{a1} = 20$, $r_{a2} = 5$, though nothing depends on this particular choice provided that r_{m1}, r_{m2}, r_{a1}, r_{a2} are sufficiently large.

Finally, before giving a list of plots, we recall that the terminology for 0th-, 1st- and 2nd-order WKB solution corresponds to the number of terms retained in the formulas (13)-(14), as described at the end of Section 4.

Another notational comment, by "classical" and "improved" WKB solutions we mean, respectively, geometrical optics solution of Section 4 and the same solution combined with either boundary-layer solution or exact solution (this will be specified in a figure title) of Section 5 in a way described in the first paragraph of the current section.

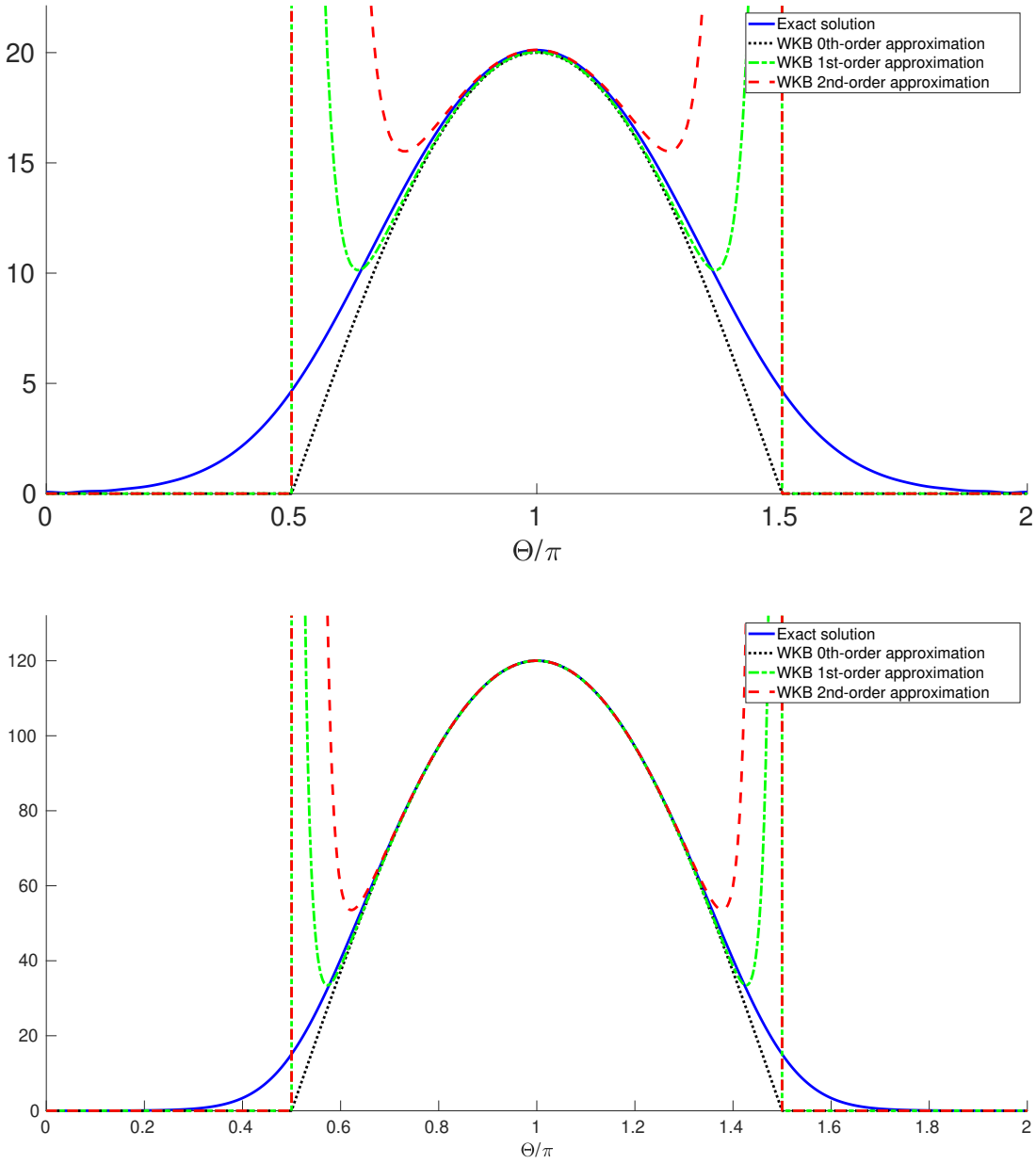

Figure 1: Comparison of classical WKB and exact solutions for $\partial_n u|_{\partial\Omega}$, $k = 10$ (top) and $k = 60$ (bottom).

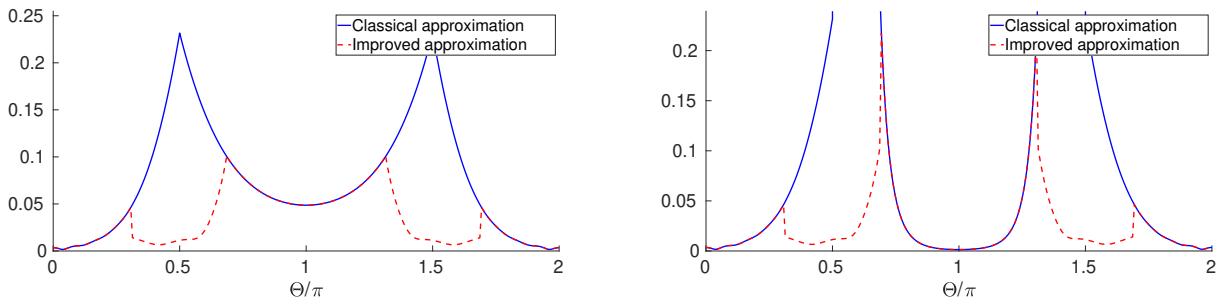

Figure 2: Relative errors in $\partial_n u|_{\partial\Omega}$ for WKB 0th-order (left) and 2nd-order (right) solution, $k = 10$.

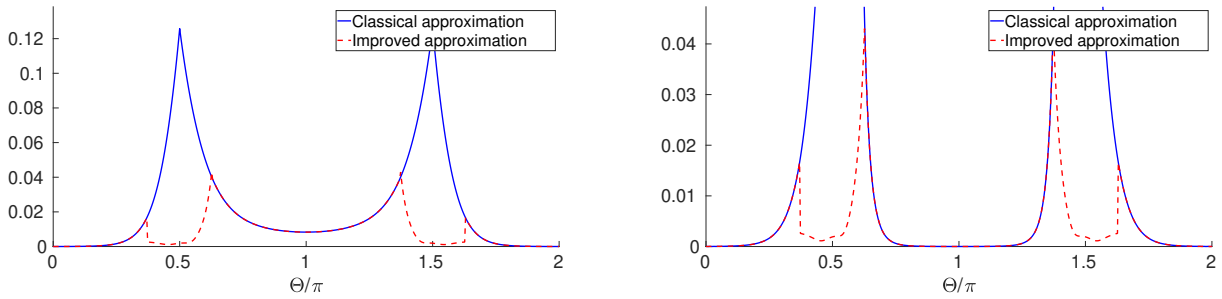

Figure 3: Relative errors in $\partial_n u|_{\partial\Omega}$ for WKB 0th-order (left) and 2nd-order (right) solution, $k = 60$.

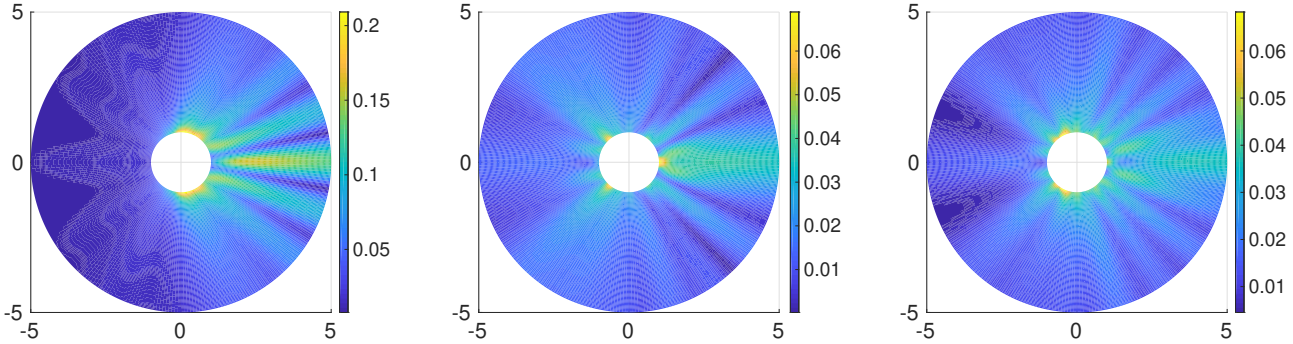

Figure 4: Relative error in u for WKB 0th-order: classical (left) and improved with exact (middle) and boundary-layer (right) solutions, $k = 10$.

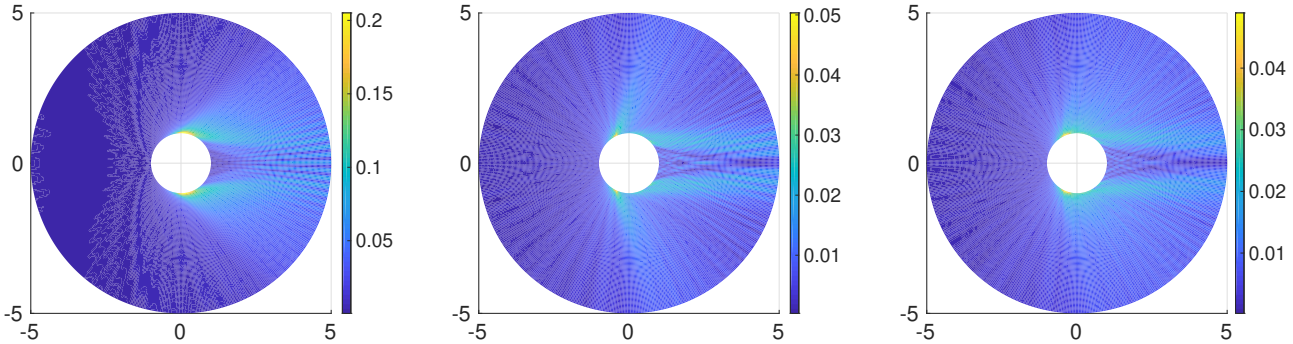

Figure 5: Relative error in u for WKB 0th-order: classical (left) and improved with exact (middle) and boundary-layer (right) solutions, $k = 60$.

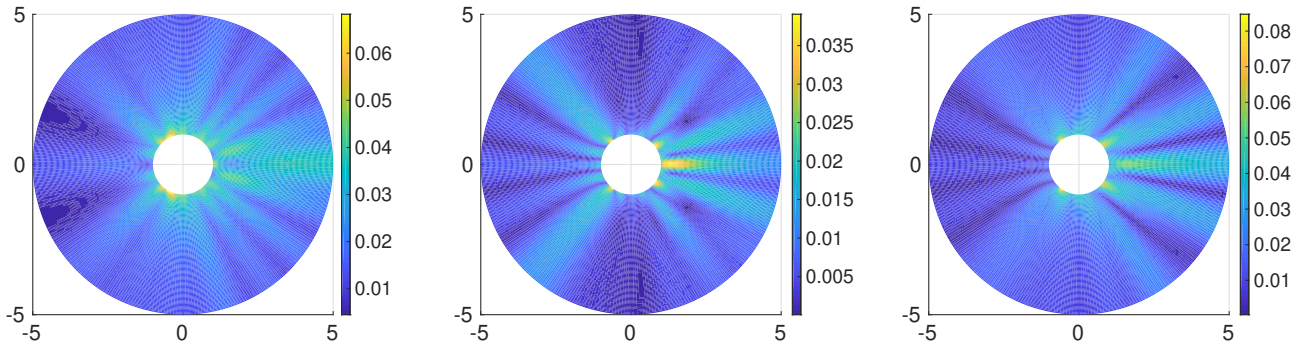

Figure 6: Relative error in u for boundary-layer improved WKB solutions: 0th order (left), 1st order (middle) and 2nd order (right), $k = 10$.

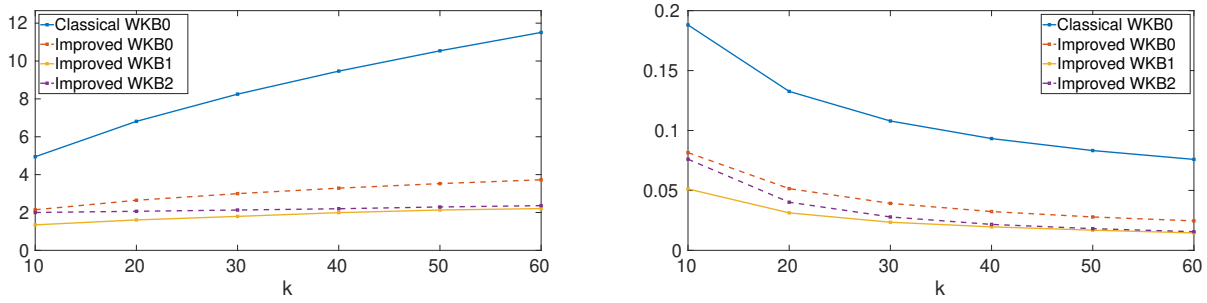

Figure 7: Absolute (left) and relative (right) $L^2(\partial\Omega)$ errors in $\partial_n u|_{\partial\Omega}$ for different k.

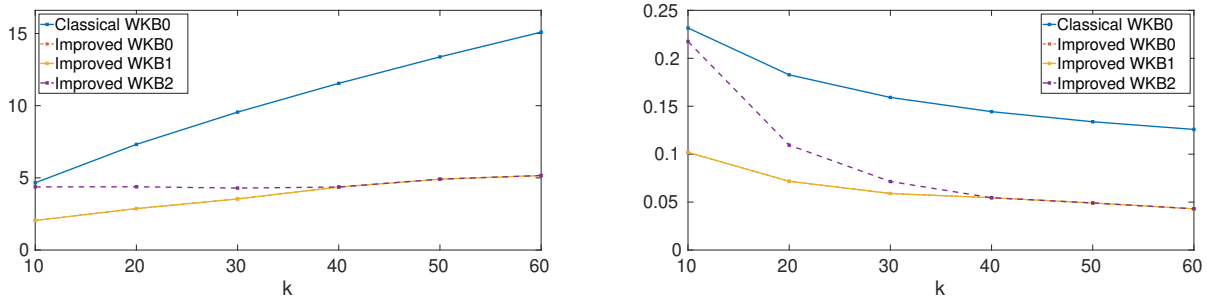

Figure 8: Absolute (left) and relative (right) $L^\infty(\partial\Omega)$ errors in $\partial_n u|_{\partial\Omega}$ for different k.

References

[1] V. M. Babich, N. Y. Kirpichnikova, "The Boundary-Layer Method in Diffraction Problems", Springer, 1979.

[2] D. Bouche, F. Molinet, R. Mittra, "Asymptotic Methods in Electromagnetics", Springer, 1994.

[3] S. N. Chandler-Wilde, I. G. Graham, "Boundary integral methods in high frequency scattering" in "Highly Oscillatory Problems" (eds. B. Engquist, A. Fokas, E. Hairer, A. Iserles), Cambridge University Press, 2009.

[4] D. L. Colton, R. Kress, "Inverse acoustic and electromagnetic scattering theory", Springer, 1992.

[5] V. Domingues, I. G. Graham, V. P. Smyshlyaev, "A hybrid numerical-asymptotical boundary integral method for high-frequency acoustic scattering", Numer. Math. 106, 471-510, 2007.

[6] R. F. Goodrich, "Fock theory", Studies in Radar Cross-Sections XXVI, 1958.

[7] D. P. Hewett, "Tangent ray diffraction and the Pekeris caret function", Wave Motion 57, 257-267, 2015.

[8] R. H. Tew, S. J. Chapman, J. R. King, J. R. Ockendon, B. J. Smith, I. Zafarullah, "Scalar wave diffraction by tangent rays", Wave Motion 32, 363–380, 2000.

[9] E. Zauderer, "Boundary layer and uniform asymptotic expansions for diffraction problems", SIAM J. Appl. Math. 19(3), 575–600, 1970.

[10] E. Zauderer, "Wave Propagation Around a Convex Cylinder", J. Math. Mech. 13, 171–186, 1964.

[11] E. Zauderer, "Partial differential equations in applied mathematics", Wiley-Interscience, 1998.